Interleukin-6 signaling promotes alternative macrophage activation to limit obesity-associated insulin resistance and endotoxemia

Jan Mauer[#], Bhagirath Chaurasia[#], Julia Goldau, Merly C. Vogt, Johan Ruud, Khoa D. Nguyen, Sebastian Theurich, A. Christine Hausen, Joel Schmitz, Hella S. Brönneke, Emma Estevez, Tamara L. Allen, Andrea Mesaros, Linda Partridge, Mark A. Febbraio, Ajay Chawla, F. Thomas Wunderlich, Jens C. Brüning

[#]These authors contributed equally to the current study

Correspondence should be addressed to J.C.B. (bruening@nf.mpg.de).

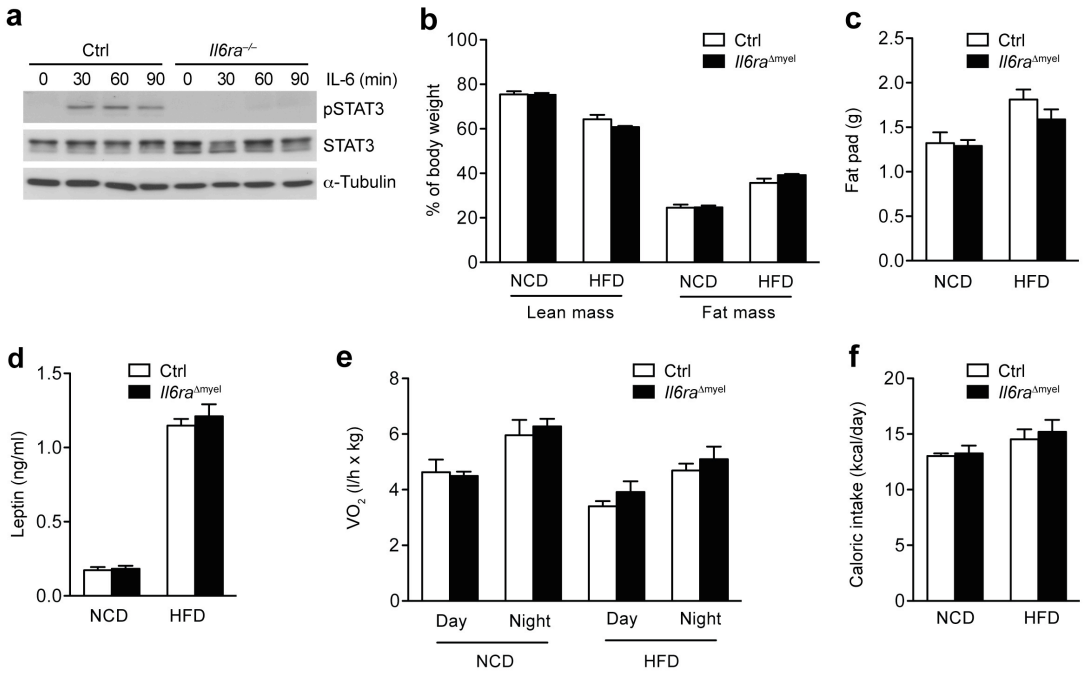

Supplementary Figure 1: Physiological characterization of NCD and HFD *Il6ra*$^{\Delta myel}$ mice. **(a)** Immunoblot of bone marrow-derived macrophages (BMDM) generated from control (Ctrl) or *Il6ra*$^{\Delta myel}$ mice (*Il6ra*$^{-/-}$) that were stimulated with IL-6 (50 ng/ml) for the indicated time points (Blot is representative of three independent experiments). **(b)** body composition (n=6), **(c)** fat pad weight (n=10), **(d)** serum leptin concentration (n=8), **(e)** oxygen (O_2) consumption (n=6) and **(f)** daily caloric intake (n=8) of normal chow diet (NCD) or high fat diet (HFD) Ctrl and *Il6ra*$^{\Delta myel}$ mice. (Values are expressed as mean ± sem)

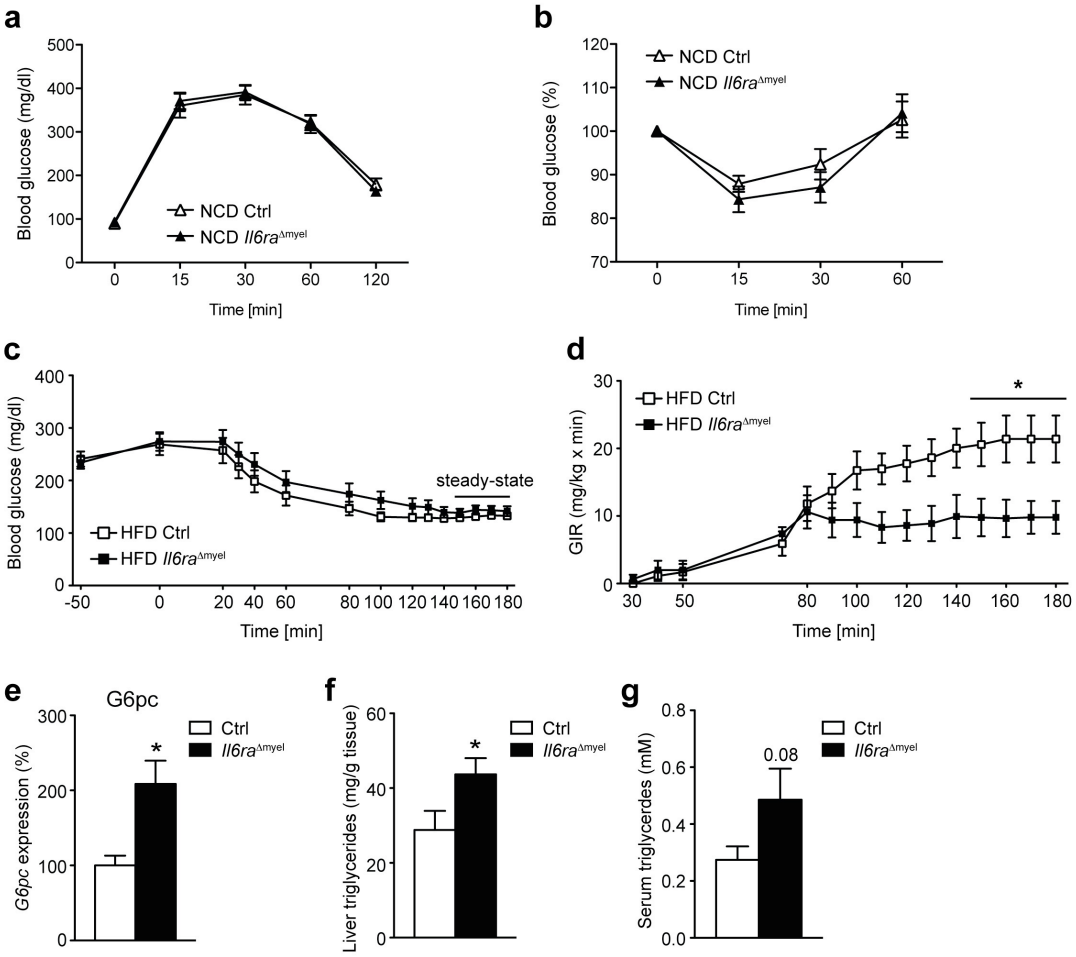

Supplementary Figure 2: Metabolic characterization of NCD and HFD *Il6ra*$^{\Delta myel}$ mice. NCD Ctrl or *Il6ra*$^{\Delta myel}$ mice were subjected to **(a)** glucose tolerance tests (GTT; n=12 vs 14) or **(b)** insulin tolerance tests (ITT; n=8 vs 14). **(c)** Blood glucose levels during euglycemic-hyperinsulinemic clamp analyses of HFD-fed Ctrl or *Il6ra*$^{\Delta myel}$ mice (n=8 vs 7). **(d)** Glucose infusion rate (GIR) during euglycemic-hyperinsulinemic clamp analyses (n=8 vs 7; *p≤0.05; 2-Way-ANOVA with Bonferroni's post-test). **(e)** qRT-PCR analyses of livers from HFD Ctrl and *Il6ra*$^{\Delta myel}$ mice that were fasted for 16 hours (n=9 *p≤0.05; unpaired student's t-test; Data is expressed as % of Ctrl). **(f)** Triglyceride content in livers of HFD Ctrl and *Il6ra*$^{\Delta myel}$ mice that were fasted for 6 hours (n=11 vs 10; *p≤0.05; unpaired student's t-test). **(g)** Triglyceride concentration in serum of HFD Ctrl and *Il6ra*$^{\Delta myel}$ mice that were fasted for 6 hours (n=11 vs 10; p=0.08; unpaired student's t-test). (Values are expressed as mean ± sem)

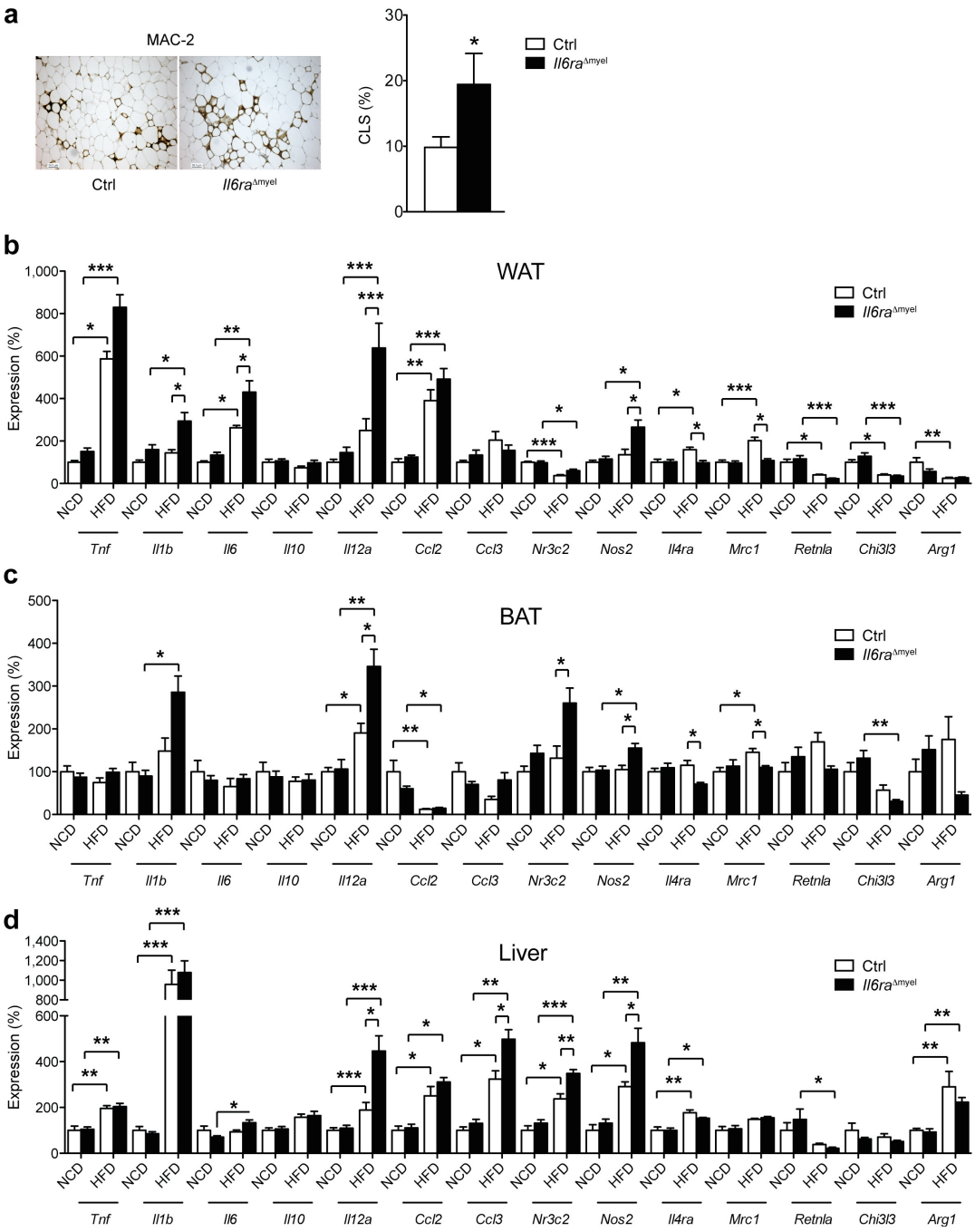

Supplementary Figure 3: Gene expression profiles in WAT, BAT and liver of NCD and HFD *Il6ra*$^{\Delta myel}$ mice. **(a)** Immunohistochemical staining of MAC2-positive cells in WAT from HFD Ctrl or *Il6ra*$^{\Delta myel}$ mice and quantification of MAC2-positive crown-like structures (CLS) in WAT from HFD-fed Ctrl or *Il6ra*$^{\Delta myel}$ mice (n=6 per genotype; *p≤0.05; unpaired student's t-test; Data is expressed as % CLS of adipocytes). **(b)** qRT-PCR analyses of WAT from NCD and HFD Ctrl or *Il6ra*$^{\Delta myel}$ mice (n=8 vs 8 NCD; n=7 vs 7 HFD; *p≤0.05, **p≤0.01, ***p≤0.001; 2-Way-ANOVA with Bonferroni's post-test; Data is expressed as % of NCD Ctrl). **(c)** qRT-PCR analyses of BAT from NCD and HFD Ctrl or *Il6ra*$^{\Delta myel}$ mice (n=4 vs 5 NCD; n=9 vs 9 HFD; *p≤0.05, **p≤0.01 vs NCD; 2-Way-ANOVA with Bonferroni's post-test; Data is expressed as % of NCD Ctrl). **(d)** qRT-PCR analyses of liver from NCD and HFD Ctrl or *Il6ra*$^{\Delta myel}$ mice (n=8 vs 8 NCD; n=9 vs 9 HFD; *p≤0.05, **p≤0.01, ***p≤0.001; 2-Way-ANOVA with Bonferroni's post-test; Data is expressed as % of NCD Ctrl). (Values are expressed as mean ± sem)

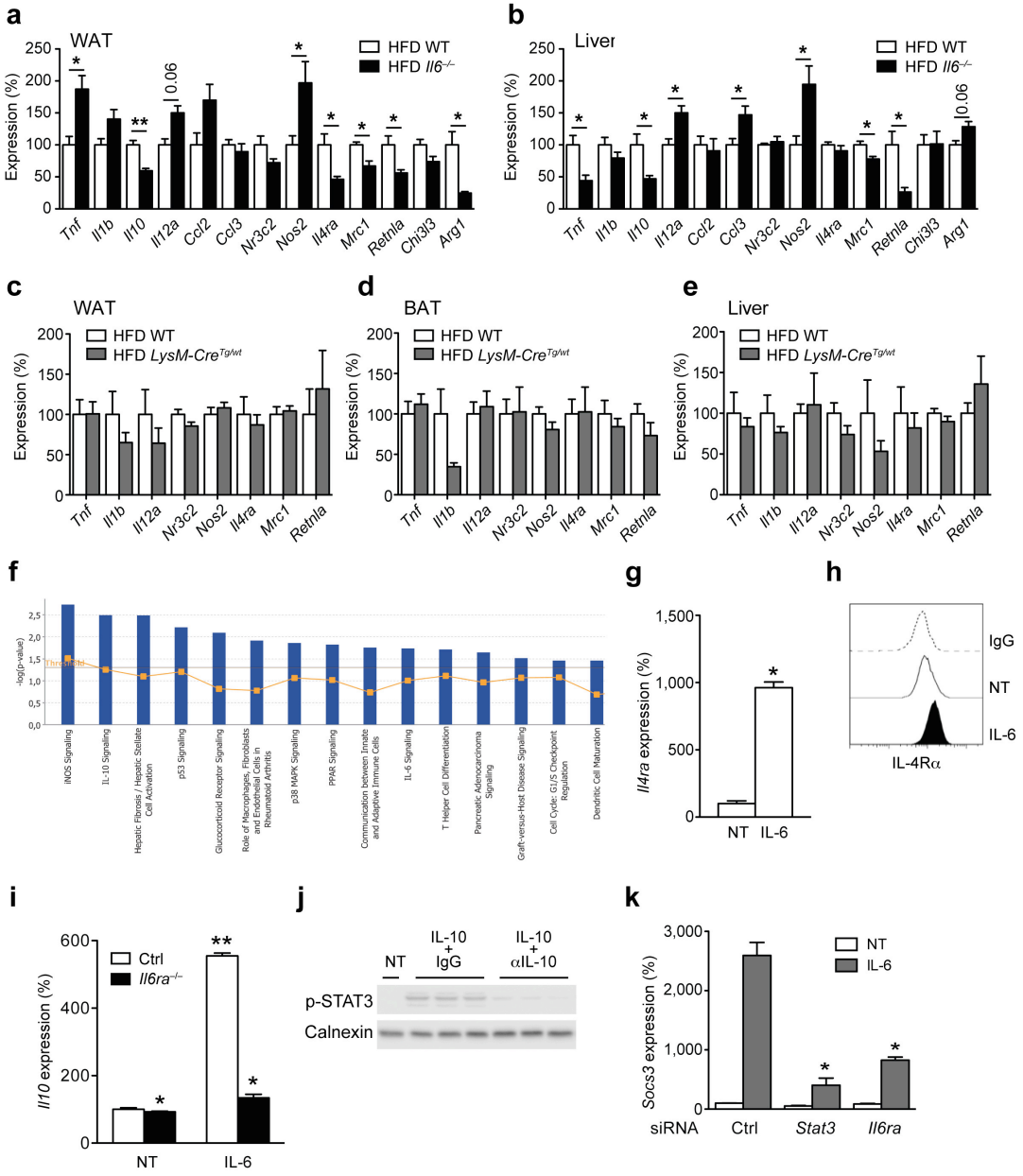

Supplementary Figure 4: Gene expression profiles in metabolic tissues of HFD *Il6*$^{-/-}$ and *LysM-Cre*$^{Tg/wt}$ mice and macrophage autonomous effects of IL-6. qRT-PCR analyses of **(a)** WAT and **(b)** liver from HFD wildtype (WT) and conventional IL-6 knockout (*Il6*$^{-/-}$) mice (n=7 vs 7 *p≤0.05, **p≤0.01; unpaired student's t-test; Data is expressed as % of WT). qRT- PCR analyses of **(c)** WAT, **(d)** BAT and **(e)** liver from HFD-fed wildtype (WT) and heterozygous *LysM-Cre* (*LysM-Cre*$^{Tg/wt}$) mice (n=5vs5; Data is expressed as % of WT). **(f)** Representative Gene ontology analyses of the 15 highest scoring canonical pathways containing gene sets that were differentially expressed between Ctrl and *Il6ra*$^{-/-}$ bone marrow-derived macrophages (BMDM) after stimulation with IL-6 (50 ng/ml; 4 hours; Threshold 0.05; Fisher's Exact t-test). **(g)** qRT-PCR analyses of in Ctrl BMDM that were left untreated or stimulated with IL-6 (50 ng/ml; 4 hours; Representative data from three independent experiments, each in triplicates; ***p≤0.001; unpaired student's t-test; Data is expressed as % of NT). **(h)** Representative FACS plots of IL-4Rα expression in Ctrl BMDM after treatment with IL-6. **(i)** qRT-PCR analyses of Ctrl or *Il6ra*$^{-/-}$ BMDM that were left untreated or stimulated with IL-6 (50 ng/ml; 12 hours) (Representative data from three independent experiments, each in duplicates; *p≤0.01 vs Ctrl; **p≤0.001 vs NT; 2-Way-ANOVA with Bonferroni's post-test; Data is expressed as % of NT Ctrl). **(j)** Immunoblot of Ctrl BMDM that were left untreated (NT) or

stimulated with IL-10 (10 ng/ml; 30 min) in the absence (IgG) or presence of an IL-10-neutralizing antibody (αIL-10) (n=3). **(k)** qRT-PCR analyses of siRNA-transfected Ctrl BMDM that were left untreated (NT) or IL-6-stimulated (4h, 50ng/ml) (n=3 independent experiments each in triplicates; *$p \leq 0.001$; 2-Way-ANOVA with Bonferroni's post-test; Data is expressed as % of NT Ctrl siRNA). (Values are expressed as mean ± sem)

a

STAT3 binding site preditions

Promoter	Site ID	Score	Relative score	Start	End	Predicted site sequence
Il4ra	*Stat3*_1	7.172	0.819	-1233	-1223	TAGCAGGAAG
Il4ra	*Stat3*_2	6.249	0.803	-1099	-1089	GTCAGGGAAG
Il4ra	*Stat3*_3	6.439	0.806	-442	-432	TGTTAGGAAA
Il4ra	*Stat3*_4	9.571	0.864	-307	-297	TGCCAGAAAG
Socs3	*Stat3*_5	7.889	0.833	-84	-74	TTACAAGAAG
Socs3	*Stat3*_6	12.671	0.921	-61	-51	TTCCAGGAAT

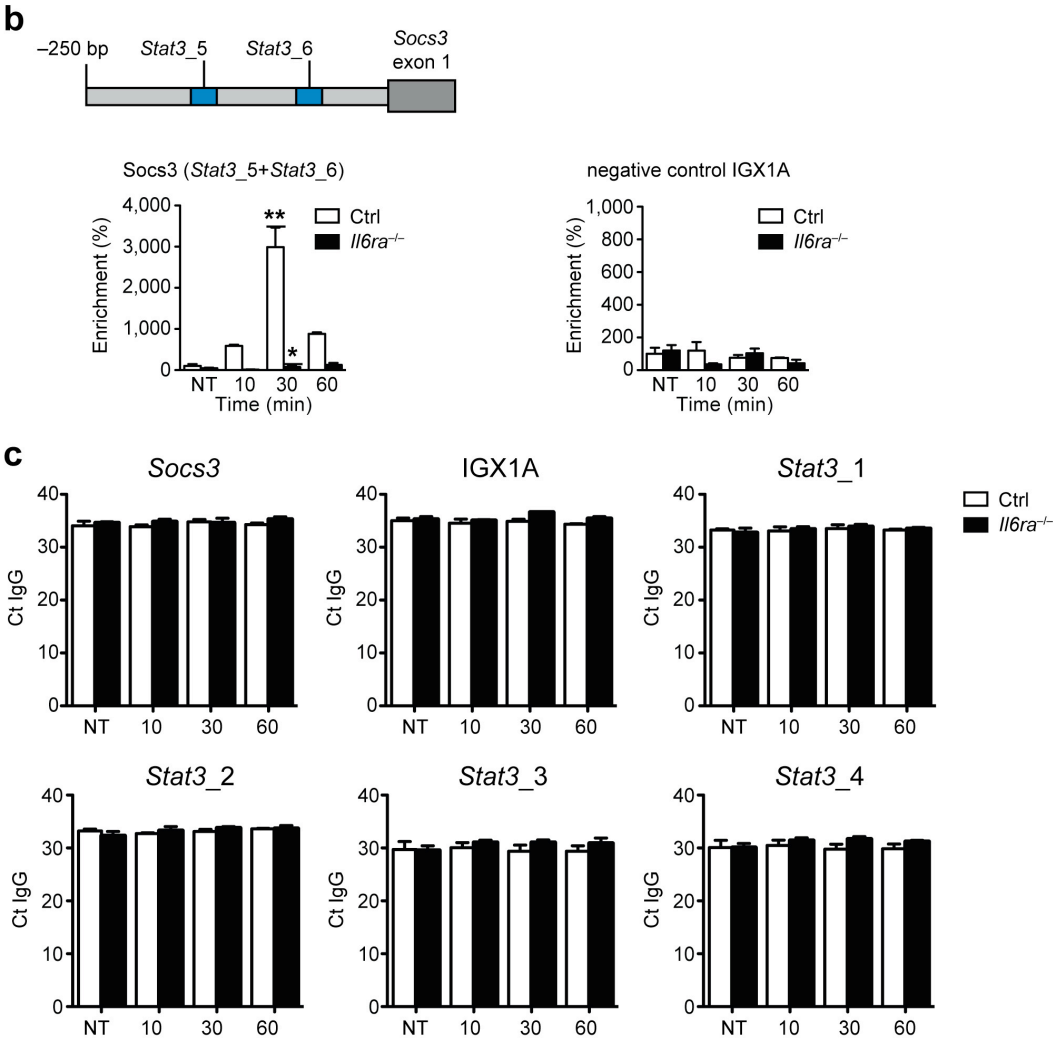

Supplementary Figure 5: STAT3 binding site prediction and ChIP analyses of IL-6 stimulated macophages. **(a)** JASPAR prediction analysis of putative STAT3-binding sites in the *Il4ra* and *Socs3* promoter **(b)** ChIP qRT-PCR showing occupancy of p-STAT3 over the *Socs3* promoter (left panel) and over a non-open reading frame region (negative control IGX1A; right panel) in Ctrl and *Il6ra*$^{-/-}$ BMDM stimulated with IL-6 (50ng/ml) for the indicated time points (n=3 vs 3 independent experiments; *p≤0.001 vs Ctrl **p≤0.001 vs NT; 2-Way-ANOVA with Bonferroni's post-test; Data is expressed as % of NT Ctrl). **(c)** qRT-PCR Cycle threshold (Ct) values obtained with the indicated primer sets on DNA samples from IgG ChIP (n=3 vs 3 independent experiments). (Values are expressed as mean ± sem)

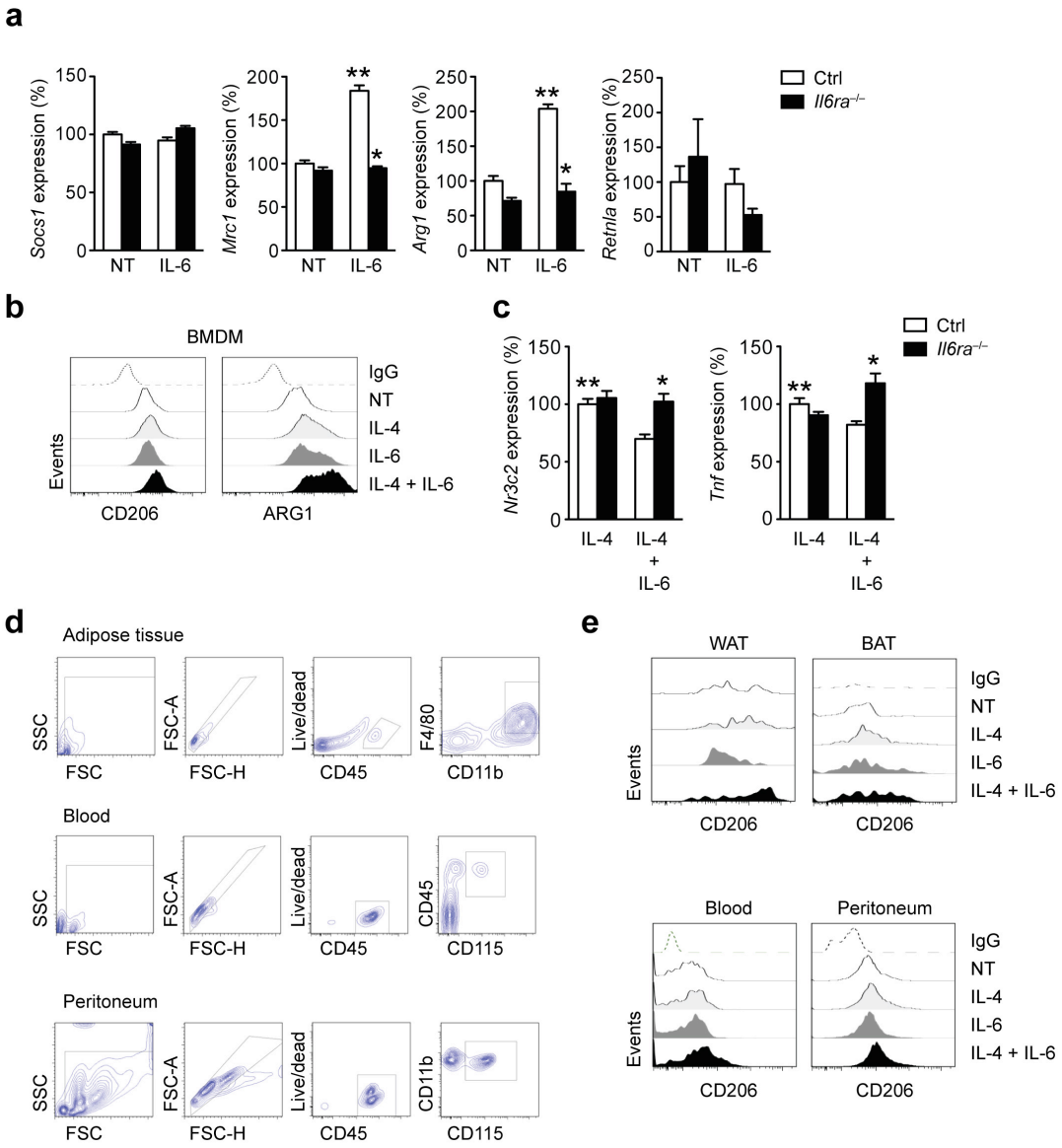

Supplementary Figure 6: Effects of IL-6 and IL-4 on macrophages *in vitro* and *in vivo*. **(a)** qRT-PCR analyses of bone marrow-derived macrophages (BMDM) from Ctrl or *Il6ra*$^{\Delta myel}$ (*Il6ra*$^{-/-}$) mice that were left untreated or stimulated with IL-6 (50 ng/ml; 12 hours) (n=6; *p≤0.01 vs Ctrl **p≤0.001 vs NT; 2-Way-ANOVA with Bonferroni's post-test; Data is expressed as % of NT Ctrl). **(b)** Representative FACS plots of expression of CD206 and ARG1 in Ctrl BMDM. **(c)** qRT-PCR analyses of Ctrl BMDM and *Il6ra*$^{-/-}$ BMDM that were left untreated or stimulated with IL-6 (50 ng/ml; 12 hours) and subsequently exposed to IL-4 (10 ng/ml) alone or IL-4 in combination with IL-6 for an additional 24 hours (n=6; *p≤0.05 vs Ctrl **p≤0.01 vs IL-4; 2-Way-ANOVA with Bonferroni's post-test; data is expressed as % of IL-4 Ctrl). **(d)** Gating strategy for FACS analysis of adipose tissue, blood, and peritoneum **(e)** Representative FACS plots of expression of CD206 in WAT, BAT, blood and peritoneal cavity of Ctrl mice. (Values are expressed as mean ± sem)

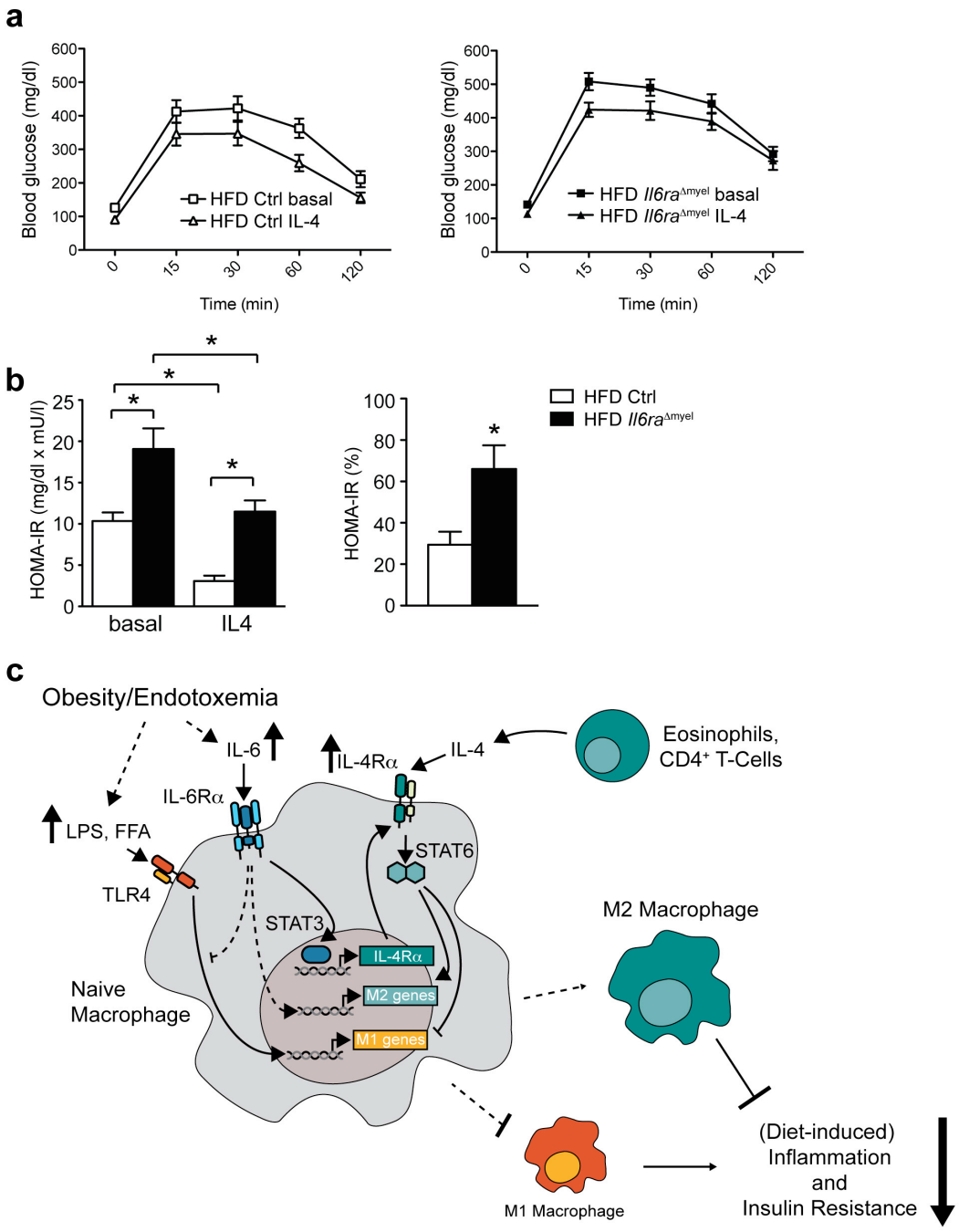

Supplementary Figure 7: Effects of IL-4 treatment in HFD *Il6ra*$^{\Delta myel}$ mice and proposed model. **(a**) Glucose tolerance tests (GTT) of HFD Ctrl (left panel) and HFD *Il6ra*$^{\Delta myel}$ mice (right panel) before (basal) and after a 4-week treatment period with IL-4 (n=15 vs 18). **(b)** (left panel) Homeostatic model assessment of insulin resistance (HOMA-IR) indices of HFD Ctrl and HFD *Il6ra*$^{\Delta myel}$ mice before (basal) and after a 4-week treatment with IL-4 (basal n=8 vs 7; IL-4 n=15 vs 18; *p≤0.01; 2-Way-ANOVA with Bonferroni's post-test). (right panel) Percentual improvement of HOMA-IR indices upon IL-4 treatment (n=8vs7; *p≤0.05; unpaired student's t-test; Data is expressed as % of basal). (Values are expressed as mean ± sem). **(c)** Proposed model: Pro-inflammatory conditions such as obesity or endotoxemia lead to increased serum concentrations of free fatty acids (FFA), bacterial lipopolysaccharides (LPS) and, among other cytokines, interleukin 6 (IL-6). FFA and LPS on one hand stimulate toll-like receptor 4 (TLR4) to activate expression of pro-inflammatory mediators such as TNFα, IL1β, IL-12 and iNOS, which are associated with classical M1 macrophage activation. IL-6 on the other hand activates STAT3 to induce expression of the IL-4 receptor. The increased

abundance of IL-4 receptors on the cell surface leads to enhanced sensitivity to IL-4, which is thought to mainly stem from eosinophils and $CD4^+$ T-cells. Binding of IL-4 to its receptor activates anti-inflammatory STAT6, which is a central transcriptional activator of factors related to alternative M2 macrophage activation, such as MRC1, ARG1, Retnla/FIZZ1 and IL-10. IL-6- and IL-4-dependent signaling cascades then act synergistically to inhibit expression of M1-associated genes and to activate M2-associated genes, ultimately tilting the balance towards increased numbers of M2 macrophages. This shift in macrophage polarization by combined IL-6- and IL-4-action finally serves to limit inflammation, to retain insulin sensitivity and to restore homeostasis during sepsis.

Supplementary Table 1: Primer pairs used for ChIP qRT-PCR:

Primer	**Sequence**
Stat3_1_fwd	CAGAGTGGTCACTTAGGAAGTCTG
Stat3_1_rev	GTCAGGACAGAGCCAAGGATAC
Stat3_2_fwd	TGCTAAGAATTCCCATCATTGTGCC
Stat3_2_rev	GAATCTAGACAGTGCTGACAGACC
Stat3_3_fwd	GCTTGCGGGCCATCTCAT
Stat3_3_rev	CTTGCTGCTACTACCAAGAG
Stat3_4_fwd	CCTGAACCTAGCAGGAGAC
Stat3_4_rev	AGCTTGGCTTGTGTTTGCG
Stat3_Socs3_fwd	CGCGCACAGCCTTTCAGTG
Stat3_Socs3_rev	TTTACCCGGCCAGTACGCC